Publications of the Astronomical Society of the Pacific
107: 32–48, 1995 January

CN and Ca Abundance Variations Among the Giants in M22

BARBARA J. ANTHONY-TWAROG,[1] BRUCE A. TWAROG,[1] AND JASON CRAIG

Department of Physics and Astronomy, University of Kansas, Lawrence, Kansas 66045-2151
Electronic mail: anthony@kuphsx.phsx.ukans.edu, twarog@kuphsx.phsx.ukans.edu

Received 1994 August 1; accepted 1994 October 28

ABSTRACT. We have obtained *uvbyCa* data for over 300 giants and horizontal-branch stars in three fields of M22. The spread in $(b-y)$ for the giant and horizontal branches is consistent with a spread in foreground reddening $\Delta E(B-V)\sim 0.08$. Reanalysis of the data of Norris and Freeman (1983a,b) indicates not only positive correlations between CH, CN, and Ca, but decidedly bimodal distributions of CH and CN and a unimodal distribution for Ca. Our photometric indices, m_1 and hk, demonstrate a range in metallicity that persists to two magnitudes below the horizontal branch, and confirm the correlation between calcium abundance and CN/CH. We infer from comparisons to spectroscopic data that m_1 is dominated by the CN and CH abundance and find no independent evidence of a range in [Fe/H]. The excessive ranges in m_1 and hk also suggest the influence of a continuous opacity source, reminiscent of the Bond-Neff effect, that is correlated with CNO abundance. The relative contributions of internal mixing and primordial variations for M22's giants are discussed.

1. INTRODUCTION

Whenever the chemical homogeneity of globular clusters is considered, ω Centauri is invariably noted as the extreme exception to almost every rule that typifies most of the Milky Way globular-cluster population. Inevitably, M22 follows as a less extreme example of a cluster with a chemical inhomogeneity that may be of primordial origin, but the comparison of M22 to ω Cen has always been a qualified one. Like ω Cen (Dickens and Woolley 1967), M22 has a substantial spread in color among its giant-branch stars, not as large but still larger than the photometric errors in $(B-V)$ (Arp and Melbourne 1959). The significance of this color dispersion has always been questionable, given the position of the cluster near the galactic center $[(l,b)=(9\overset{\circ}{.}9,-7\overset{\circ}{.}6)]$ and early estimates of high foreground reddening (e.g., Hesser 1976) which suggested the possibility of reddening variations across the cluster area. However, Crocker (1988), using spectroscopic measurements of the Balmer strengths of six blue-horizontal-branch stars, constrained the total range in $E(B-V)$ to be less than 0.08 mag. A similar conclusion was reached by Minitti et al. (1992) based on polarization measures. Additional confirmation of the modest spread in reddening across the field of M22 has been provided by Bates et al. (1992), who find from an analysis of *IRAS* images that $\Delta E(B-V)\sim 0.05$.

Direct attempts to measure elemental abundance variations have been frustratingly inconclusive. In ω Cen, the color spread among the giants is large, as is the spread in [Fe/H], and the two are correlated—the more metal-rich stars, on average, are redder at a given V magnitude. The smaller range in color within M22 could be interpreted as an indicator of a narrower range in [Fe/H], reddening variations aside. The strongest photometric evidence for a spread in [Fe/H] comes from the DDO survey by Hesser et al. (1977), but the identification of all of the metal-rich M22 stars as nonmembers (see Sec. 5.3) eliminates this option. Unfortunately, with the exception of Laird et al. (1991), the pattern of spectroscopic studies has been one of small samples; as a result, the occasional detections of a range in [Fe/H] in M22 appear, at best, marginally significant. For a review of these analyses, see Lehnert et al. (1991, hereafter referred to as LBC). If there is a spread in [Fe/H] among the giants in M22, it would appear to be no larger than 0.2 dex.

In sharp contrast with [Fe/H], a large number of studies (e.g., Hesser et al. 1977; Hesser and Harris 1979; Lloyd Evans 1978; Frogel et al. 1983) have consistently concluded that CNO elements show a wide range of variation in M22. For purposes of detailing the sizes and possible correlations of these variations within the cluster and relative to other clusters, the large sample in the survey by Norris and Freeman (1983a,b; hereafter collectively referred to as NF) has given this study unusual importance in the discussion. From a sample of 100 bright giants, NF found a significant spread in CN, CH, and, surprisingly, Ca, with all three elemental indicators positively correlated. CN and CH variations among globular-cluster giants are not rare; in the most intriguing cases with bimodal distributions, CN and CH are anticorrelated, as might be expected if they are the product of some form of mixing phenomenon involving CN-processed material during stellar evolution. However, NF claimed no indication of bimodality among the giants in M22 and such CN processing provides no mechanism for linked variations in Ca, usually an indicator of primordial effects.

The purpose of this paper is to present the results of a CCD survey of the giant branch of M22 on the *uvbyCa* system. The reasons for this particular photometric, rather than spectroscopic, approach to the problem are numerous. First, despite the apparent strong interest in this question, there is no CCD-based color–magnitude diagram (CMD) for M22, broadband or otherwise. Since one of the key observational constraints on homogeneity, or lack thereof, within a cluster is the spread in observed color among supposedly similar stars, this seemed a minimal first step. Second, the spectroscopic studies to date have been limited to small samples and stars well above the horizontal branch. With a CCD and a

[1]Visiting Astronomer, Cerro Tololo Inter-American Observatory, a division of the National Optical Astronomy Observatories, which is operated by the Association of Universities for Research in Astronomy, Inc. (AURA), under contract with the National Science Foundation.

TABLE 1
Log of CCD Observations

Filter	Expos. Time	U.T.	Date	Filter	Expos. Time	U.T.	Date
		Southwest				**South**	
y	15	06:00:11	28-Jun-92	y	15	00:47:06	17-Oct-92
y	45	06:03:24	28-Jun-92	y	45	00:49:16	17-Oct-92
y	45	06:04:51	28-Jun-92	y	45	00:50:48	17-Oct-92
b	40	06:06:45	28-Jun-92	y	45	08:26:08	28-Jun-92
b	120	06:08:17	28-Jun-92	y	45	08:27:40	28-Jun-92
b	120	06:10:59	28-Jun-92	b	40	00:52:56	17-Oct-92
v	120	06:14:14	28-Jun-92	b	130	00:55:17	17-Oct-92
v	360	06:17:15	28-Jun-92	b	130	00:58:10	17-Oct-92
v	360	06:23:51	28-Jun-92	b	120	08:26:08	28-Jun-92
u	150	06:30:51	28-Jun-92	v	120	01:01:42	17-Oct-92
u	600	06:35:07	28-Jun-92	v	360	01:04:45	17-Oct-92
u	600	06:45:43	28-Jun-92	v	360	01:11:32	17-Oct-92
Ca	200	06:57:17	28-Jun-92	v	360	08:35:10	28-Jun-92
Ca	600	07:04:15	28-Jun-92	v	360	08:42:00	28-Jun-92
Ca	600	07:48:23	28-Jun-92	u	150	01:18:25	17-Oct-92
				u	150	00:49:41	18-Oct-92
		Northeast		u	600	01:21:50	17-Oct-92
y	45	09:31:24	07-Jun-91	u	600	00:56:48	18-Oct-92
y	45	09:32:44	07-Jun-91	u	600	08:49:00	28-Jun-92
y	45	09:34:12	07-Jun-91	u	600	09:00:00	28-Jun-92
b	120	09:22:36	07-Jun-91	Ca	150	00:07:51	18-Oct-92
b	120	09:25:12	07-Jun-91	Ca	150	00:22:18	18-Oct-92
b	120	09:27:54	07-Jun-91	Ca	600	00:27:12	18-Oct-92
v	360	09:01:47	07-Jun-91	Ca	600	00:37:52	18-Oct-92
v	360	09:08:22	07-Jun-91	Ca	600	08:03:56	28-Jun-92
v	360	09:15:04	07-Jun-91	Ca	600	08:14:47	28-Jun-92
u	540	08:04:53	07-Jun-91				
u	540	08:14:29	07-Jun-91				
u	540	08:24:11	07-Jun-91				
Ca	480	08:35:06	07-Jun-91				
Ca	480	08:43:42	07-Jun-91				
Ca	480	08:52:24	07-Jun-91				

telescope of modest aperture, the photometric approach allows us to increase the sample from a few dozen to a few hundred, reaching two magnitudes below the horizontal branch, an important gain if one is looking for the potential effects of stellar evolution on the giant branch. Third, studies involving large samples of metal-deficient field giants (Bond 1980; Twarog and Anthony-Twarog 1991; Pilachowski et al. 1993; Anthony-Twarog and Twarog 1994) have demonstrated the value of the *uvbyCa* system for disentangling the fundamental properties of halo giants. The use of both m_1 and hk provides two independent means of estimating [M/H] based primarily upon Fe and Ca, respectively. Fourth, a series of papers applying CCD intermediate-band photometry to NGC 6397 (Anthony-Twarog 1987; Anthony-Twarog et al. 1992), ω Cen (Mukherjee et al. 1992), and Mel 66 (Anthony-Twarog et al. 1994) has shown that the precision required by such systems is readily attainable. In the case of M22, as with ω Cen and Mel 66, the nature of the questions under consideration makes the internal precision of the photometry much more important than the accuracy of the zero-point link to an external system.

The outline of the paper is as follows: Sec. 2 will detail the observations, their reduction, and the accuracy of the photometric indices. In Sec. 3 the cluster CMD is analyzed and an attempt made to place constraints on the possible range in reddening across the fields in the survey. A reanalysis of the sample of NF will be given in Sec. 4 as a prelude to the extensive analysis of the photometric indices in Sec. 5. Section 6 contains a summary of our conclusions and possible options for future work.

2. THE OBSERVATIONS

2.1 Reduction and Calibration

Three fields in M22, designated NE, SO, and SW, were imaged through *uvbyCa* filters with the Cassegrain CCD camera ($f/7.5$) on the 1.5-m telescope at Cerro Tololo Inter-American Observatory in 1991 and 1992. The frame log is given in Table 1. The CCD frames were initially processed at the telescope using standard IRAF routines; the frames were not averaged in preparation for aperture and profile-fitting photometry. At the University of Kansas, all frames described in Table 1 were processed with the DoPHOT photometric reduction package described by Schechter et al. (1993). Instrumental magnitudes from similar frames were collated and averaged using software described in Anthony-Twarog et al. (1994). Our collating software provides instrumental photometric indices, each with its own internal error based on the standard deviation of multiple measurements of each filter-magnitude. We took the additional step of employing the overlap between the SO and SW fields to merge indices from these two fields to a common instrumental system.

We invoked a composite of techniques to determine the transformation equations relating the DoPHOT-derived indices to the *uvyCa* system. In conjunction with the frames

TABLE 2
Comparison of Photoelectric to CCD Index Values

AM ID	ID	V_{HHM}	Photoelectric Values V	$b-y$	m_1	c_1	hk	CCD Values V	$b-y$	m_1	c_1	hk
I-57	51170	11.92						11.950				
I-62	51169		12.041	0.526	0.084	0.379	0.521	12.057	0.520	0.046	0.455	0.510
I-75	51171		11.873	0.806	0.318	0.412	1.037	11.924	0.345	0.370	0.370	1.037
I-80	51172	12.54	12.548	0.904	0.281	0.445	0.955	12.481	0.908	0.292	0.413	0.965
I-81	50030	13.67						13.666				
I-82	50055	13.67						13.775				
III-79	40006	13.03						13.108				
III-81	40004		13.077	0.652	0.041	0.442	0.603	13.067	0.610	0.094	0.417	0.679
III-109	40002	11.63	11.702	0.803	0.362	0.487	1.164	11.711	0.845	0.312	0.502	1.088
IV-34	20024	14.39						14.366				

described in Table 1, we obtained frames and aperture photometry of stars on the adopted standard system defined by Bond (1980) to determine the *form* of the calibration equations relating instrumental to standard values. We then employed photoelectric photometry of several M22 giants to determine the *zero-points* of the calibration equations. Where possible, we also obtained aperture photometry of M22 giants on the same nights as standard stars, but our calibration equations are most strongly tied to photoelectric photometry obtained on the CTIO 1.5-m telescope in June and August of 1991 as part of a program to observe field halo giants on the *uvbyCa* system. The observations were carried out and reduced as detailed in Anthony-Twarog and Twarog (1994) and Anthony-Twarog et al. (1991); the *uvby* data are consistent with the system of Bond (1980) for red giants. The hk indices have been transformed to the standard system of Anthony-Twarog et al. (1991) as part of the compilation of the catalog of observations on the Ca system described in Twarog and Anthony-Twarog (1995).

The slopes of the calibration equations were determined separately for the runs in 1992 October and 1991 June. Five halo field giants on the adopted standard *uvbyCa* system were observed with the CCD on 1992 October 17. Aperture magnitudes within 14-pixel radii were constructed from the data using IRAF routines; extinction coefficients for all five filters were determined by a series of observations of a standard star over a wide range of airmass. The calibration equations for this night relate observed to standard values for V, $(b-y)$, m_1, c_1, and hk with standard errors of 0.004, 0.003, 0.009, 0.014, and 0.014, respectively.

For the 1991 June run, none of the nights on which frames of M22 were taken was photometric. However, we have characterized the form of the calibration equations for the 1991 June data based on similar CCD observations of eleven halo field giants on the adopted standard *uvbyCa* system obtained on an adjacent night, 1991 June 8. For these eleven stars the dispersion of the residuals about the calibration relation amounted to 0.012, 0.006, 0.018, 0.018, and 0.019 for V, $(b-y)$, m_1, c_1, and hk, respectively.

Finally, given the slopes of the equations relating our instrumental photometric indices to standard values, we appealed to direct comparison of the adjusted instrumental values for five stars in the NE and SO/SW fields to the photometric values based on our 1991 observations to set the zero-points. For *uvby*, we included information based on the additional step of aperture measurements of several uncrowded stars in the SO field from frames obtained on the night of 1992 October 17. The final calibration equations for the photometric nights during the two runs are:

JUNE 1991

$$V=0.992y_i+0.021(b-y)_i+z_y,$$
$$(b-y)=1.10(b-y)_i+z_{by},$$
$$m_1=0.944m_{1i}-0.12(b-y)_i+z_{m1},$$
$$c_1=1.078c_{1i}+0.21(b-y)_i+z_{c1},$$
$$hk=1.019hk_i+z_{hk}$$

OCTOBER 1992

$$V=1.005y_i+0.023(b-y)_i+z_y,$$
$$(b-y)=1.152(b-y)_i+z_{by},$$
$$m_1=0.999m_{1i}-0.11(b-y)_i+z_{m1},$$
$$c_1=1.094c_{1i}+0.30(b-y)_i+z_{c1},$$
$$hk=0.992hk_i+z_{hk}.$$

Table 2 summarizes the comparisons between our calibrated CCD photometry and photoelectric indices; the comparison of our DOPHOT-based photometry for these stars to photoelectric values provides a fairly optimistic view of the zero-point errors of our calibration.

Table 2 also contains V magnitudes from other sources as well; we have photoelectric V magnitudes for seven stars from Hesser et al. (1977). For these stars, the difference in V magnitude in the sense (PE$-$CCD) is -0.030 ± 0.061. There are other photometric sources with which to compare our V magnitudes. We also compared V to several large photographic surveys, including those of Alcaino (1977) and Peterson and Cudworth (1994). These two comparisons are linked since the calibration of the latter photographic study is tied to standards in the former. For 169 red giants and blue-horizontal-branch stars in common with Peterson and Cudworth (1994), the difference in V magnitudes in the sense (PC$-$CCD) is -0.09 ± 0.06. A separate comparison to Alcaino (1977) gives a virtually identical result, a difference (AL$-$CCD) of -0.09 ± 0.08. While most of these comparisons imply CCD-derived magnitudes that are faint with respect to photographic values, we have applied the greatest

TABLE 3
uvbyCa Photometry of M22 Stars[a]

I.D.	AM ID	AL ID	Memb. Prob.	X	Y	V	$b-y$	m_1	c_1	hk	σ_V	σ_{by}	σ_{m1}	σ_{c1}	σ_{hk}	Num. Frames				
																y	b	v	u	Ca
21307				-35.7	-106.8	11.118	1.245	0.302	0.839	1.273	0.000	0.000	0.000	0.139	0.024	1	1	1	3	2
51168	I-92	1.78	88	125.2	99.3	11.571	1.071	0.215	0.701	1.133	0.000	0.002	0.004	0.006	0.004	1	3	3	3	3
40002	III-109	3.81	0	-96.7	-327.8	11.711	0.845	0.312	0.502	1.088	0.012	0.029	0.040	0.033	0.042	3	2	3	3	2
21308				108.5	-110.5	11.885	1.058	0.114	0.792	0.961	0.005	0.006	0.007	0.011	0.008	3	2	3	3	4
51171	I-75	2.56	0	176.5	150.0	11.924	0.807	0.345	0.370	1.037	0.001	0.003	0.005	0.006	0.004	2	3	3	3	3
51170	I-57	1.72	99	193.3	61.5	11.950	1.059	0.338	0.492	1.293	0.002	0.002	0.003	0.003	0.010	2	3	3	3	3
21309	IV-20		93	23.8	-106.9	12.044	1.082	0.291	0.646	1.148	0.011	0.017	0.026	0.053	0.028	3	2	3	4	4
51169	I-62	2.46	0	218.5	84.7	12.057	0.520	0.046	0.455	0.510	0.004	0.005	0.006	0.006	0.005	2	3	3	3	3
32813	III-11	3.82	0	-57.3	-309.7	12.107	0.985	0.478	0.518	1.376	0.003	0.005	0.007	0.007	0.008	4	6	6	7	5
20003	III-33	1.40	99	-56.8	-156.1	12.243	0.972	0.124	0.712	0.927	0.005	0.005	0.005	0.008	0.008	3	1	1	4	4
50023	I-86	1.86	99	109.9	159.8	12.291	0.962	0.160	0.579	0.915	0.004	0.004	0.004	0.004	0.005	3	3	3	3	3
50024	I-27		97	88.0	81.9	12.373	0.819	0.132	0.960	0.668	0.003	0.004	0.009	0.341	0.007	3	3	3	3	3
21310	III-35		31	-51.4	-134.8	12.375	0.955	0.090	0.678	0.807	0.000	0.000	0.000	0.027	0.025	1	1	1	2	2
51173	I-113	2.61	99	149.2	178.5	12.425	0.939	0.143	0.577	0.888	0.002	0.002	0.004	0.005	0.007	2	3	3	3	3
51174	I-85	1.87	99	119.5	180.7	12.455	0.868	0.110	0.594	0.759	0.002	0.003	0.006	0.008	0.005	2	3	3	3	3
51172	I-80	2.64	99	164.4	237.3	12.481	0.908	0.292	0.413	0.965	0.009	0.009	0.010	0.007	0.010	2	3	3	3	3
42816	III-86	2.18	99	-165.9	-162.9	12.506	0.853	0.264	0.449	0.963	0.021	0.025	0.039	0.042	0.050	2	2	3	3	2
50009	I-68	2.51	98	254.4	144.1	12.516	0.939	-0.008	0.599	0.617	0.006	0.010	0.013	0.009	0.013	3	3	3	3	3
42815	III-39	1.37	99	-90.3	-173.3	12.577	0.924	0.094	0.677	0.854	0.014	0.016	0.018	0.011	0.021	2	3	3	3	2
32814	IV-31	1.49	99	31.5	-219.7	12.618	0.914	0.192	0.542	0.927	0.012	0.016	0.020	0.018	0.020	7	7	8	9	8
21311				122.4	-132.5	12.632	1.016	0.040	0.729	0.791	0.011	0.014	0.020	0.022	0.017	3	2	3	3	4
50012	I-58	1.70	99	211.2	50.1	12.666	0.756	-0.049	0.774	0.395	0.003	0.003	0.004	0.008	0.004	3	3	3	3	3
21315				-56.1	-104.4	12.682	0.860	0.037	0.949	0.663	0.000	0.000	0.000	0.331	0.024	1	1	1	2	2
50020				132.4	152.5	12.717	0.754	0.117	0.633	0.484	0.033	0.034	0.035	0.016	0.034	3	3	3	3	3
51175	I-54	1.74	93	162.1	53.3	12.763	0.889	0.191	0.457	0.942	0.002	0.002	0.003	0.007	0.005	2	3	3	3	3
50010	I-116	2.43	97	237.4	53.6	12.779	0.853	0.009	0.651	0.585	0.005	0.006	0.007	0.005	0.006	3	3	3	3	3
21312				53.1	-119.4	12.868	0.859	0.021	0.676	0.650	0.002	0.005	0.012	0.030	0.012	3	2	3	4	4
20005	IV-40	2.32	99	77.4	-226.5	13.006	0.952	0.148	0.387	0.713	0.017	0.031	0.054	0.059	0.040	5	4	5	6	6
40005	III-78	2.23	98	-115.8	-243.2	13.046	0.899	0.230	0.459	0.900	0.009	0.013	0.018	0.019	0.018	3	3	3	3	2
40004	III-81	2.26	0	-109.5	-216.0	13.067	0.610	0.094	0.417	0.679	0.008	0.012	0.018	0.023	0.015	3	3	3	3	2

[a]Table 3 is presented in its complete form in the ApJ/AJ/PASP CD-ROM Series, volume 4, 1995. A portion of the table is presented here for guidance regarding the content and format of the full table.

weight to our own photoelectric comparisons and have not adjusted the V magnitudes.

Table 3 presents a portion of the entire sample of calibrated CCD photometry with standard errors of the mean for each photometric index and the number of frames contributing to each index; the entire data file is presented in the CD-ROM and is also available electronically if requested of the authors. Our own five-digit running numbers indicate the field by the first digit: 5 for the NE field, 2 for the SO field, 4 for the SW field, and 3 for the region of overlap between the SO and SW fields. We have included membership probabilities from Peterson and Cudworth (1994); cross identifications to the surveys of Arp and Melbourne (1959), noted by roman numerals indicating the quadrant; Alcaino and Liller (1983), noted by ring prefixes 1 to 3; and Peterson and Cudworth (1994), noted by a preceding C. Figure 1 is a synthetic chart corresponding to the sample of stars brighter than $V=16$, where the symbol size indicates the brightness. Our on-chip coordinates have been transformed to the coordinate system of Peterson and Cudworth (1994). The X,Y positions listed in Table 3 correspond, as in Cudworth (1986), to coordinates running in arcsecond units in the positive α and δ directions from a central position of $18^{\mathrm{h}}33^{\mathrm{m}}21.5^{\mathrm{s}}$ and $-23°56'44''$, epoch 1950.

2.2 Internal Precision

One of the primary concerns in the analysis of any sample, particularly when searching for inhomogeneity, is the internal precision of the data. As noted above, magnitudes for each star in each filter are derived separately and averaged, producing an internal error estimate based upon the dispersion in the multiple CCD frames. For each index these standard errors of the mean have been combined to derive a standard error for the index. The stars have been binned by magnitude in 0.5 mag intervals and the average standard error calculated for each index; the resulting trend is seen in Fig. 2. For all of the indices the average standard error grows slowly down to $V=16$, where a more rapid increase occurs. Moreover, the dispersion in the standard errors of the mean (s.e.m.) increases significantly. Note also that the brightest bin exhibits larger than average errors due to the saturation effects among the brightest images and the smaller number of frames on which these stars could be processed. To ensure that the analysis of the photometric sample is dominated by real effects as opposed to photometric errors, in future discussion of the indices we will limit the sample to stars brighter than $V=16$ with s.e.m.$_V \leq 0.04$, s.e.m.$_{b-y} \leq 0.06$, and s.e.m. for m_1, c_1 and $hk \leq 0.08$.

3. THE COLOR–MAGNITUDE DIAGRAM

The CMD for 956 stars brighter than $V=17.0$ is presented in Fig. 3(a). The primary features of the giant branch and the blue horizontal branch are well defined, though there is evidence for a color spread among the giants and modest contamination from field stars. To help clarify the picture a bit, we have applied the standard error cuts listed in Sec. 2.2,

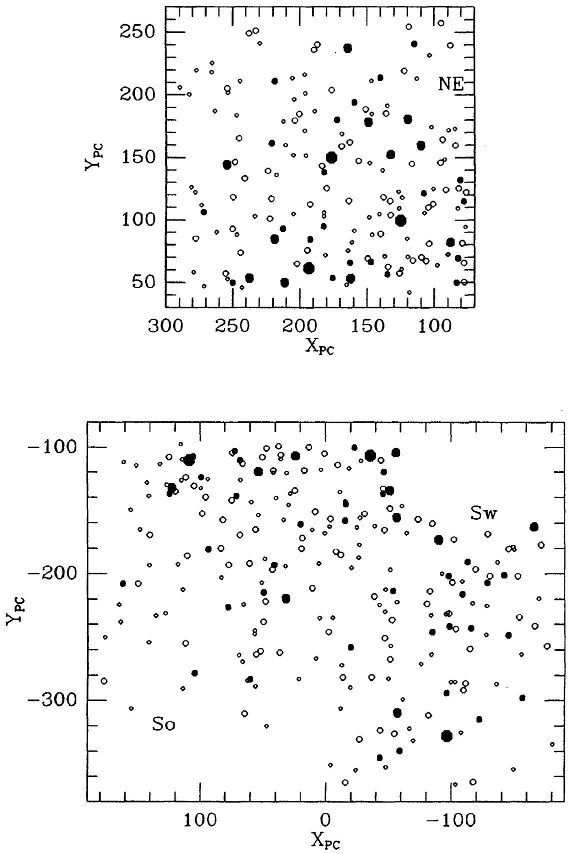

FIG. 1—Synthetic chart of our three fields in M22, showing positions of stars to approximately $V=16.0$. Larger and filled symbols denote brighter stars. The X, Y coordinates are on the system of Peterson and Cudworth (1994).

decreasing the sample to 396 stars above $V=16.0$, of which 20% appear to populate the blue horizontal branch. An additional cut can be made using the proper-motion membership study of Peterson and Cudworth (1994), eliminating all stars with membership probabilities below 80%. The CMD based upon the distilled sample is shown in Fig. 3(b) where filled circles identify all stars with membership probabilities greater than 80% and open circles are stars for which membership information does not exist.

The effect of the proper-motion study is apparent. Above the approximate completeness limit of the survey, the majority of the stars scattered to the red of the giant branch in Fig. 3(a) have disappeared. While some scatter is still present blueward of the giant branch, it should be remembered that above the level of the horizontal branch near $V \sim 14.0$, asymptotic giant branch stars will be present and these will lie blueward of the first-ascent giant branch. The sharp distinction in membership for stars redward of the giant branch permits an additional selection criterion for the analysis sample in Sec. 5: we will consider stars to be photometric nonmembers, even if they lack proper-motion data, if their colors are more than 0.15 mag redder than the mean color of the giant branch at the same V magnitude.

Fainter than $V=13.0$, the branch is reasonably narrow and can be used to place constraints on potential variations in reddening and metallicity within the sample. Using only stars classed as members, a mean relation has been drawn through the points on the first-ascent giant branch between $V=16$ and 13. For each point, the residual in $(b-y)$ relative to the mean relation was calculated and the histogram of the resulting residuals fit to a Gaussian. Excluding points that are more than three sigma away from the mean, the standard deviation of the $(b-y)$ residuals about the mean curve from 61 points is found to be ± 0.031 mag. This dispersion comes from three sources: photometric errors, a reddening spread, and a metallicity spread. For the same 61 points, the average standard error of the mean in $(b-y)$ is found to be 0.009 mag, leaving a combined effect due to reddening and metallicity of ± 0.030 mag. If we assume that all of the residual spread is due to reddening, this leads to an upper limit on $E(B-V)$ of ± 0.04 mag, in excellent agreement with the studies noted in Sec. 1.

No known RR Lyrae variables are located within our survey field. The horizontal branch is well defined by the probable members shown in Fig. 3(b) where the red edge of the blue horizontal branch appears to be $(b-y)=0.38$. Barring evolutionary anomalies, these BHB stars are too hot to show the effects of variable metallicity on $(b-y)$ or $(B-V)$. The width of the BHB in color is comparable to the width of the giant branch, and can be attributed to a modest spread in $E(b-y)$, consistent with the results for the giants. To further verify this, we constructed unreddened $[m_1]$ and $[c_1]$ indices for the BHB stars, looking for any distinctive characteristics among the reddest or faintest BHB stars in the $[m_1]$, $[c_1]$ plane. The redder BHB stars mix indistinguishably with the other BHB stars, and we were unable to identify any distinctive populations within our sample.

4. NORRIS AND FREEMAN (1983a,b) REVISITED

One of the key questions in discussions of M22 is the degree of similarity between M22 and the *typical* globular cluster. M22's reputation for being a unique cluster is due in large part to the work of NF. Since one of the purposes of this investigation is to build upon and expand the analysis of M22 by NF, it is critical that the new data sample be tied as tightly as possible to the earlier data and that both are analyzed in as similar a fashion as possible. In their classic study of M22's red giants, NF synthesized three indices for approximately 100 red giants with probable memberships based on their radial velocities. One index, A(Ca), is similar to our *hk* index and samples the absorption due to the Ca II H and K lines at 3933 and 3966 Å. $S(3839)$ measures the strength of the CN band that begins at 3883 Å, and W(G) measures the strength of the G band, a prominent CH feature near 4300 Å; W(G) is available for only about half the full sample.

NF examined possible correlations among all three of these abundance parameters as well as the distribution functions for each index. NF calculated δ forms for $S(3839)$ and A(Ca); δS, for example, is constructed as $S-S(V)$, where S is the observed S index and $S(V)=1.065-0.09V_{\rm NF}$, the predicted value for *normal* stars in the cluster at the observed V.

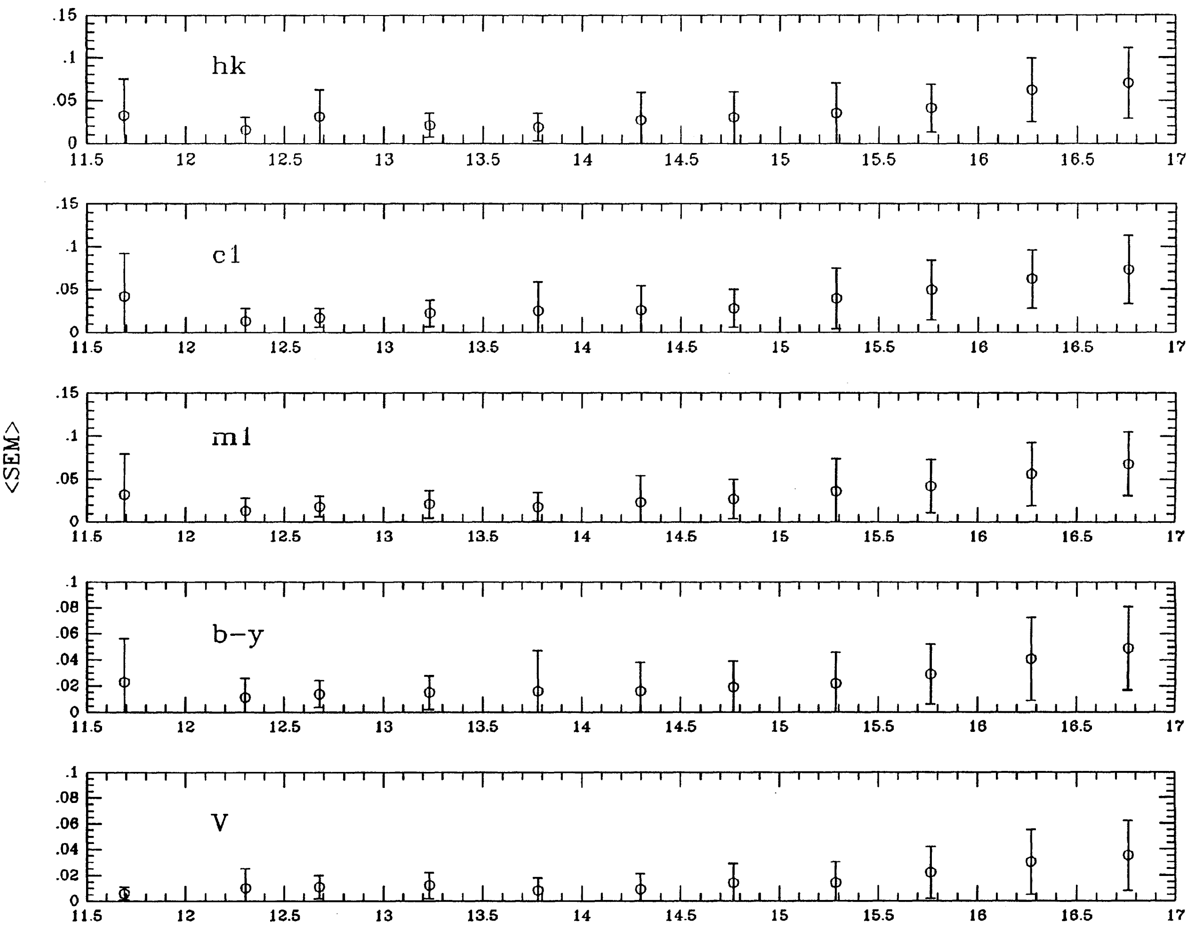

FIG. 2—Instrumental errors in $(b-y)$, m_1, c_1, and hk as a function of V magnitude. The average s.e.m. in each 0.5 mag bin is plotted, with error bars indicating the range of s.e.m. values in each bin.

As defined, stars with larger δS indices have higher CN absorption than other stars at the same magnitude. A similar relation is available for A(Ca). We have extended this notion and calculated δW(G) parameters from the NF data, using a fiducial relation $W(\mathrm{G})=23.42-1.25V_{\mathrm{NF}}$. Implicit in these relations is the assumption that stars at the same V are in the same evolutionary phase and should have the same intrinsic $(B-V)$. Because the scatter in V caused by photometric errors and/or a reddening spread is small compared to the slopes of the relations, a spread in the differential indices is more likely to be the result of true star-to-star differences than one tied to color-based fiducial relations.

NF noted positive correlations among all three of their indices, but stopped short of characterizing M22 as a bimodal cluster, perhaps because the distinction between the CN-rich and CN-poor stars was not as sharp as in their more canonical example of a bimodal cluster, NGC 6752. To place the analysis on somewhat less subjective ground, we have employed the KMM mixture-model algorithm (Ashman et al. 1994) to explore the presence and significance of multiple peaks in the distribution of each of the three NF photometric parameters. Among other diagnostic statistics, the KMM program returns a probability, P, which is a measure of the improvement of a multimode fit to the data over a single Gaussian model. P-values <0.05 represent significant rejections of single-mode Gaussian fits to the distribution function. P-values between 0.05–0.10 represent marginal rejections of the unimodal hypothesis.

A histogram of the δA(Ca) looks like a Gaussian distribution, characterized by a peak near $\delta A(\mathrm{Ca})=-0.01$ and a σ-width of $\sim$0.03. The KMM algorithm confirms the estimates of the mean and width, and returns a large P-value, implying that a two-group model does **not** provide a statistically significant improvement over a single Gaussian model, consistent with the interpretation reached by LBC of a unimodal distribution of δA(Ca) values. In strong contrast, as summarized in Table 4, the KMM analysis finds two groups in the distributions of δS and δW(G) that are highly significant, with peaks that are separated by amounts significant with respect to the random errors in the indices themselves. The algorithm also determines the mixing ratios between the two populations, indicated in Table 4 as

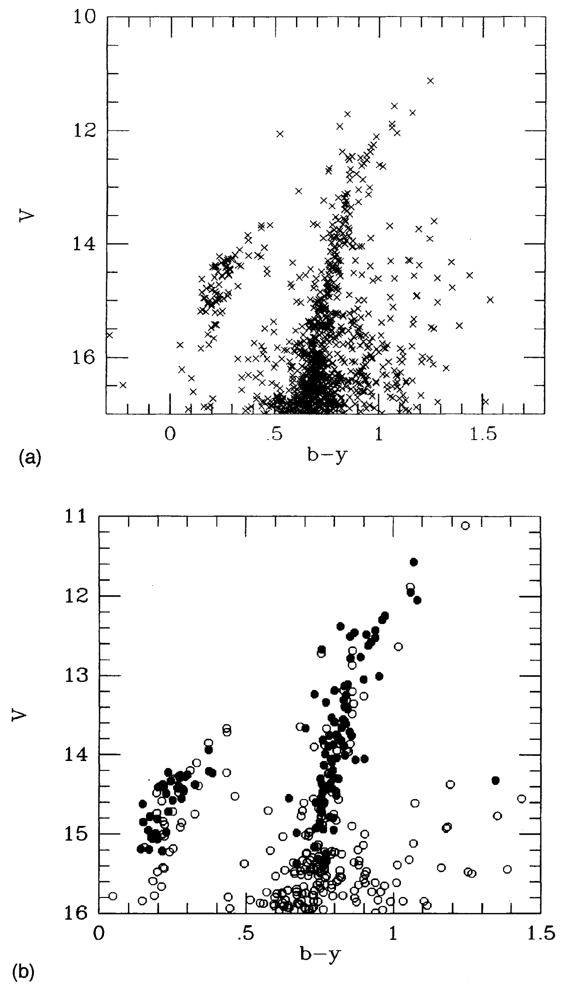

FIG. 3—Color–magnitude diagrams of M22. (a) shows the entire sample of photometry to $V=17.0$. (b) is restricted to stars brighter than $V=16.0$, with nonmembers and stars with large photometric errors removed. Stars with confirmed membership are shown with filled symbols.

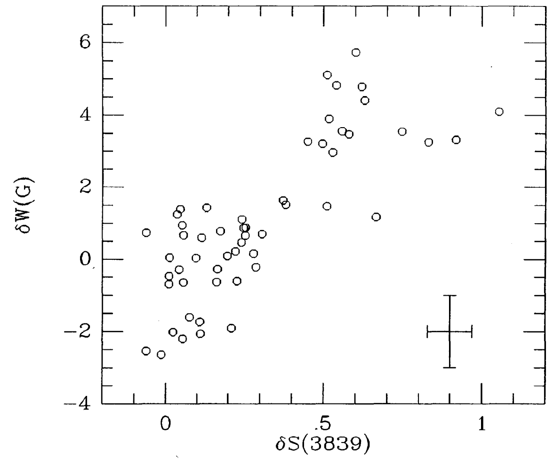

FIG. 4—δS and δW(G) indices from Norris and Freeman (1983a,b). Stars with large δS indices, indicating higher CN abundance, also have large δW(G) indices, indicating high CH abundance. Error bars indicate uncertainty in NF's spectrophotometric indices.

percentages of the total sample, based upon the probability that a star is a member of either mode in the distribution. Detailed comparison of the individual probabilities reveals that there is an almost exact correspondence between the probability classification for both indices, i.e., stars classed as members of the high δS mode are also classed as members of the high δW(G) mode. This point is illustrated graphically in Fig. 4, emphasizing one of NF's conclusions, that CH and CN are *positively* correlated in M22. However, as the KMM analysis also shows, the distribution exhibits a strong simultaneous separation between the high-CH/CN stars and the weaker CH/CN stars. If one imposes a cut in δS where the KMM placed the break between the two groups at $\delta S=0.4$, stars above this value are classed as CN/CH strong and stars below as CN/CH weak. In Fig. 5 we plot δA(Ca) vs. δW(G). In agreement with the KMM analysis, the distribution of δA(Ca) values is continuous. However, the distinction between the CN/CH strong and CN/CH weak stars is almost total in that the CN/CH strong stars all fall in the large δA(Ca) region of the diagram while none of the CN/CH weak stars populate this region.

We conclude from this analysis that while all three indices

TABLE 4
Shape and Mixture Model Parameters for Spectrophotometric Indices

Quantity	Mean of Distribution	Variance	P	Mixture Proportions
δA(Ca)	-0.01	0.03	0.21	
δW(G)	0.03	1.32	0.03	73 , 27
δW(G)	4.07	0.86		
δS	0.12	0.11	0.00	65 , 35
δS	0.60	0.21		

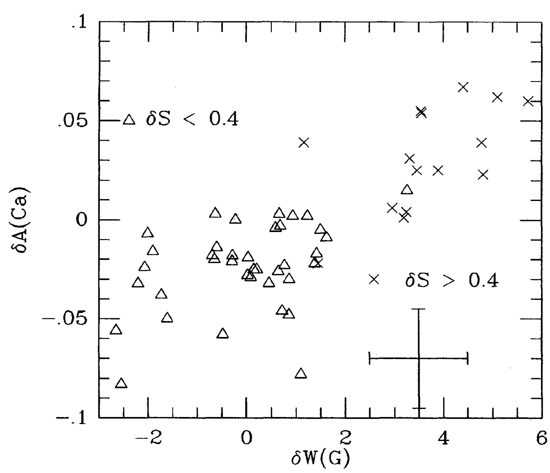

FIG. 5—δA(Ca) and δW(G) indices for the NF sample, with different symbol types indicating δS greater than or less than 0.4.

are positively correlated, as found by NF, the correlations among the three indices are not all linear. By this we mean that the distribution in Ca is large, real, and unimodal, but the spreads in CN and CH are large, real, and bimodal. The mechanism which produces the CN enhancement is also responsible for the CH enhancement, but does not affect Ca. However, the mechanism which produces the CN/CH enhancement appears to operate preferentially on stars which are Ca rich. We now turn to the larger photometric sample to see if it confirms or contradicts these interpretations.

5. THE *uvbyCa*–CCD RED-GIANT SAMPLE

In addition to the standard temperature index $(b-y)$, the *uvbyCa* system provides three primary indices: m_1, c_1, and hk. Because m_1 and c_1 share the v bandpass and are more familiar to most observers, we will begin our analysis with the discussion of these two indices. For purposes of the analysis, when needed, we will adopt an absolute reddening value of $E(B-V)=0.42$ for M22 (Crocker 1988), equivalent to $E(b-y)=0.30$.

5.1 The m_1 and c_1 Indices

To minimize the problems with photometric errors, the sample has been limited to those stars meeting the criteria of Sec. 2.2, excluding proper-motion and photometric nonmembers. For metal-poor red giants, the m_1 and c_1 indices are measures primarily of [Fe/H] and of luminosity, respectively. The metallicity sensitivity is tied to the collective changes in a number of moderate-to-weak Fe lines in the 4100 Å region covered by the v filter. The luminosity sensitivity of the c_1 index is built upon the size of the Balmer jump; for metal-deficient red giants this effect is minimal for cooler stars and changes in c_1 are more strongly linked to temperature effects in the ultraviolet. Among the hotter red giants, however, the surface gravity sensitivity is still extant, as is apparent in the separation of horizontal-branch and bluer asymptotic giant-branch stars from first-ascent giants (Bond 1980; Anthony-Twarog and Twarog 1994).

Though the traditional approach for converting m_1 to [Fe/H] uses a comparison of the observed index to a standard relation at a given color to derive a δm_1, we will instead follow the lead of NF and define δm_1 as the difference at a given V. As with the CN, Ca, and CH indices, this minimizes the effect of the photometric errors and the reddening spread while eliminating any possible secondary effects due to luminosity changes along the giant branch. Figure 6(a) contains the m_1, V distribution for the 220 stars meeting the selection criteria; the solid line represents the mean relation against which one measures δm_1. The dispersion in m_1 caused by a range of ± 0.04 in $E(B-V)$ is approximately ± 0.01. It is clear that the range in m_1 at a given V is typically an order of magnitude larger than this. Error bars illustrating a range of twice the average standard error of the mean in m_1 are also presented in Fig. 6(a). The scatter in Fig. 6(a) might be partly the result of the inclusion of a few AGB stars, but is not the result of photometric errors.

Taking into account the larger number of stars at fainter V and the increase in the photometric errors at fainter V, it appears from Fig. 6(a) that the range in δm_1 remains constant between $V=12$ and 16. This is surprising in that the mean color of the giant branch over the same magnitude range changes from $(b-y)_0=0.67$ to 0.40. The metallicity sensitivity of m_1 changes by nearly a factor of 3 over the same color range in the [Fe/H] range of -1.3 to -2.0, in the sense that a given spread in [Fe/H] produces a smaller spread in m_1 as $(b-y)_0$ decreases (Anthony-Twarog and Twarog 1994). This is the first indication that things are not what they seem; for the present, no adjustment will be made to the calculated δm_1 indices to correct for the varying sensitivity with color.

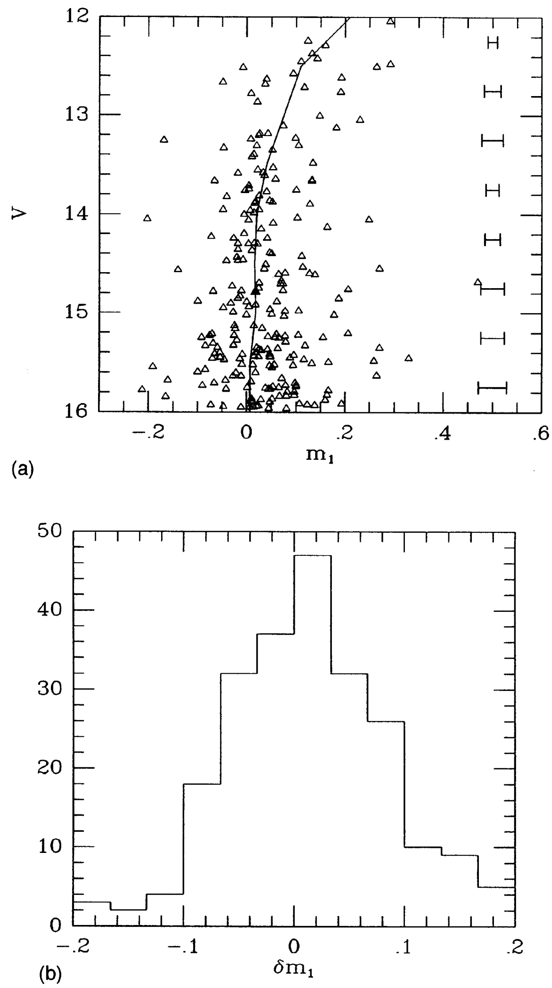

FIG. 6—V and m_1 for the restricted giant branch sample described in the text. The mean giant-branch relation is shown, as are error bars indicating typical photometric s.e.m. at various luminosity levels on the giant branch. (b) shows the distribution function of δm_1 values for this sample.

Figure 6(b) shows a histogram of δm_1 values for the 220 stars between $V=12$ and 16.0. We have removed the contribution from photometric error, about 0.03 mag, from the observed Gaussian σ, 0.09, of the δm_1 distribution to determine a true dispersion of 0.08; we will refer to 0.16, the two-*sigma* estimate of the δm_1 range in the following discussion. For stars with $V=13$, the slope of the δ[Fe/H]/δm_1

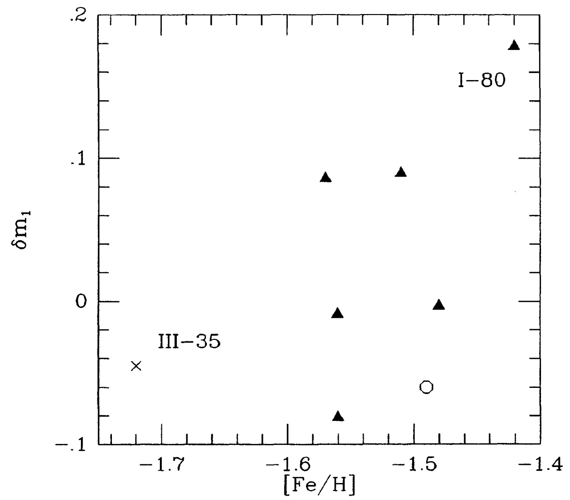

FIG. 7—Photometric indices δm_1 for stars in common with the high dispersion-spectroscopic study by LBC, plotted against their [Fe/H]. Open circle denotes star III-25, which has no proper-motion information, cross denotes star III-35, a probable nonmember based on proper motions.

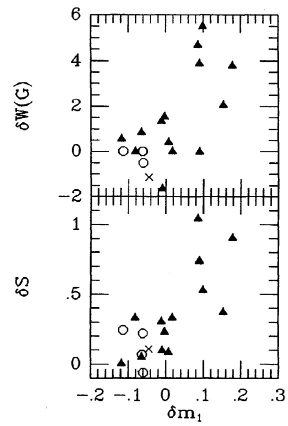

FIG. 8—Photometric metallicity index m_1 compared with NF's CN and CH indices, δS and δW(G). As for Fig. 7, open circles denote a lack of proper-motion data, crosses denote nonmembers.

relation is almost exactly 10 but increases to 20 by $V=16$. If δm_1 is truly measuring [Fe/H], the minimum spread in [Fe/H] is 1.0 dex near $V=13$, increasing to at least 2.0 dex among the fainter giants. This answer is implausible even given the range in [Fe/H] found among all the spectroscopic studies of M22 to date. If we focus on the one high-dispersion spectroscopic study with the largest sample, LBC, the possibility that m_1 is measuring variations in [Fe/H] becomes even more remote. Figure 7 illustrates δm_1 for eight stars from LBC with spectroscopic [Fe/H] determinations. One star, noted by a cross, is a proper-motion probable nonmember while a second star (open circle) does not have proper-motion data. Excluding the nonmember, the range in [Fe/H] is less than 0.2 dex, consistent within the errors with no spread in [Fe/H]. Despite the small range in [Fe/H], δm_1 covers a spread between 0.2 and 0.3 mag, equivalent to a spread of over 1.5 dex in [Fe/H].

If m_1 is not a measure of [Fe/H], what is the source of the spread at a given V? Given the location of the v filter, two options come to mind, CH and CN. The CN band at 4215 Å falls within the v filter and significant variation in CN strength should affect the m_1 index. The value of the m_1 index in identifying CN anomalies in solar-abundance red giants was demonstrated by Gustafsson and Bell (1979) using synthetic indices constructed from theoretical stellar atmospheres with enhanced nitrogen. The head of the G band is located beyond the bandpass of the v filter, but theoretical models have shown that changes in carbon abundance can change the m_1 indices through the effect of the CH continuous absorption coefficient on the v band (Tripicco and Bell 1991; Briley et al. 1993). Direct observations of CH-strong stars have regularly shown (e.g., Luck and Bond 1982) that the m_1 indices of such stars are too large and that the normal calibrations overestimate the metallicity by between 0.5 and 1.0 dex. Whether CN or CH is the root cause, it is clear that the m_1 anomalies come about through the v bandpass, since may of these same stars have anomalous c_1 indices as well, with c_1 discrepancies about twice the size of the differential in m_1 (e.g., Bond 1980; Luck and Bond 1991).

Support for the claim that m_1 is measuring CN/CH variations among M22's red giants is given in Fig. 8 where we show the trends in δm_1 as a function of (a) δS and (b) δW(G) for the overlap of stars with NF. Symbols have the same meaning as in Fig. 7. δm_1 correlates positively in some sense with both indices, such that stars in the stronger CN/CH group also have larger δm_1 values. For two reasons, it is impossible to say whether this indicates a linear correlation with CN/CH indices at all δm_1 values, or simply scatter about the two peaks in a bimodal sample. First, the scatter among the indices in either of the groups is only a factor of two larger than the individual error bars. Second, though we justifiably declined to include a color-dependent adjustment to δm_1 based upon the sensitivity of the index to [Fe/H], we have no knowledge of whether or not the sensitivity to changes in CN/CH is color dependent. It should be further emphasized that because of the unique correlation between CN and CH abundances in M22, it is impossible to say which of the two molecules dominates the effect on m_1.

We now turn to the c_1 index. From field-star data at comparable metallicity, the expectation is that c_1, $(b-y)$, and V should be correlated enough to allow reliable estimation of the cluster reddening (Anthony-Twarog and Twarog 1994). As is apparent from Fig. 9(a), analogous to Fig. 6(a), the anomalies in M22 make any such expectations meaningless. The δc_1 distribution for the 220 red giants between $V=12$ and 16 is shown in Fig. 9(b) and the range is significantly larger than that due to reddening ($<\pm 0.01$ mag) and to photometric errors. In Fig. 10, δc_1 is plotted against δm_1; the solid line illustrates a slope of -2.0. It is clear that the predominant source of the scatter within both indices must be the v filter.

5.2 The *hk* Index

The *byCa* system was devised by Anthony-Twarog et al. (1991) to fill a specific need within the Strömgren system. At

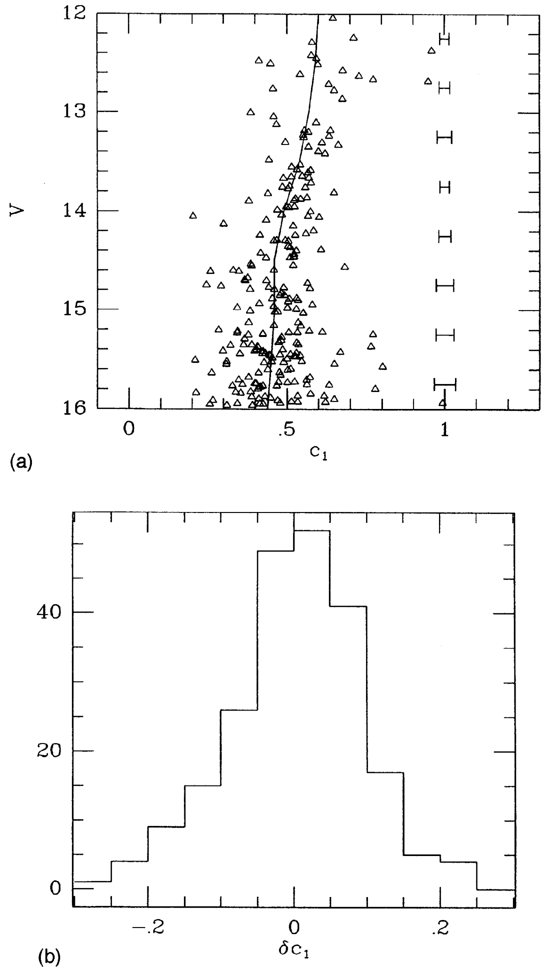

FIG. 9—As for Fig. 6, but for the c_1 index.

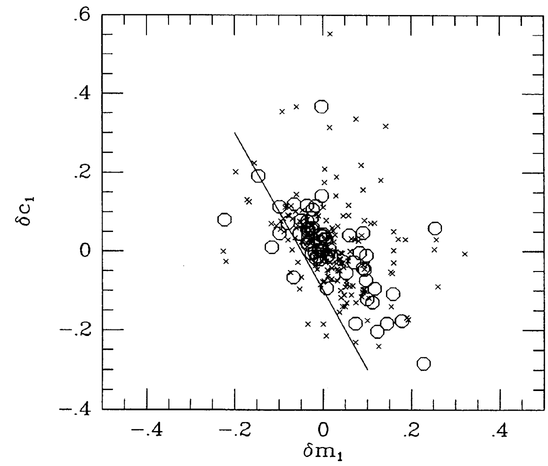

FIG. 10—For the restricted giant branch sample, plot of δc_1 vs. δm_1. Larger symbols denote stars with proper motions indicating membership—no proper-motion information exists for the stars with cross symbols. The reference line in the figure has a slope of -2.0.

low [Fe/H] the metallicity sensitivity of the m_1 index declines dramatically, particularly for hotter stars (e.g., Schuster and Nissen 1989; Twarog and Anthony-Twarog 1991). As the available sample of very metal-deficient stars has grown (Beers et al. 1985, 1992), this weakness has hindered the use of the traditional *uvby* system. To overcome this problem, a filter centered on the Ca II lines at 3933 and 3966 Å was constructed to replace the v filter in the m_1 index, creating a new index hk, sensitive to the [Ca/H] abundance rather than [Fe/H]. Because of the strength of the Ca II lines, they maintain their sensitivity to Ca variations for stars with [Fe/H] as low as -3.5, and should be applicable to stars down to -4.5. At a typical red-giant color, hk is two to three times more sensitive to changes in [m/H] than m_1, results confirmed qualitatively by Soon et al. (1993) and quantitatively by Twarog and Anthony-Twarog (1991).

Figure 11(a) shows the trend in hk as a function of V for the restricted sample of giants in M22; the solid line is the mean relation while the dispersion caused by photometric errors at each magnitude level is noted. The spread caused by the range in reddening is less than ± 0.005 mag, an indication of the weak dependence of hk on reddening. As with m_1, the scatter is real and not the result of photometric errors. After calculating δhk relative to the mean relation in Fig. 11(a), we must apply a correction to the index to account for the varying sensitivity as a function of color. Unlike m_1, we know of little else except Ca that can influence the strength of the hk index so such an adjustment is appropriate (see Sec. 5.3 for a possible exception to this claim). A renormalization constant was derived for all magnitudes between $V=12$ and 16 by calculating the renormalization as a function of color and linking that to V using the mean relation between V and $(b-y)_0$ for the M22 giant branch. Using the giant-star calibration of hk in Twarog and Anthony-Twarog (1991) near the metallicity of M22, the change in hk for a given change in [Fe/H] should be twice as large for giants near $V=12.0$ as it is for stars at $V=16.0$. Note that the revised δhk values, identified as $\delta hk'$, are defined such that the renormalization constant is 1.0 for the faintest stars, but compresses δhk for brighter stars. Figure 11(b) presents the histogram of the adjusted $\delta hk = \delta hk'$ for the stars between $V=12$ and 16. Keeping in mind the likely contamination of the fainter sample by nonmembers, the distribution is clearly unimodal. If we clip the distribution to exclude the points in the extended wings more than three sigma away from the mean, the distribution is well fit by a Gaussian with a one-sigma dispersion of ± 0.09. After removing the spread caused by photometric scatter, the two-sigma width of the remaining distribution is 0.16 mag. Using the preliminary calibration of the hk system for metal-poor red giants (Twarog and Anthony-Twarog 1991), this range translates into a range in [Ca/H] of $\geqslant 0.8$ dex, with no significant difference between the bright and faint giants.

Combining our results for m_1 and hk, we get the trend illustrated in Fig. 12. Open symbols are proper-motion members, predominantly brighter than $V=15$ while crosses are stars without membership information, mostly fainter than $V=14$. Focusing first on the members, the stars show a strong correlation between δm_1 and $\delta hk'$ in the sense that

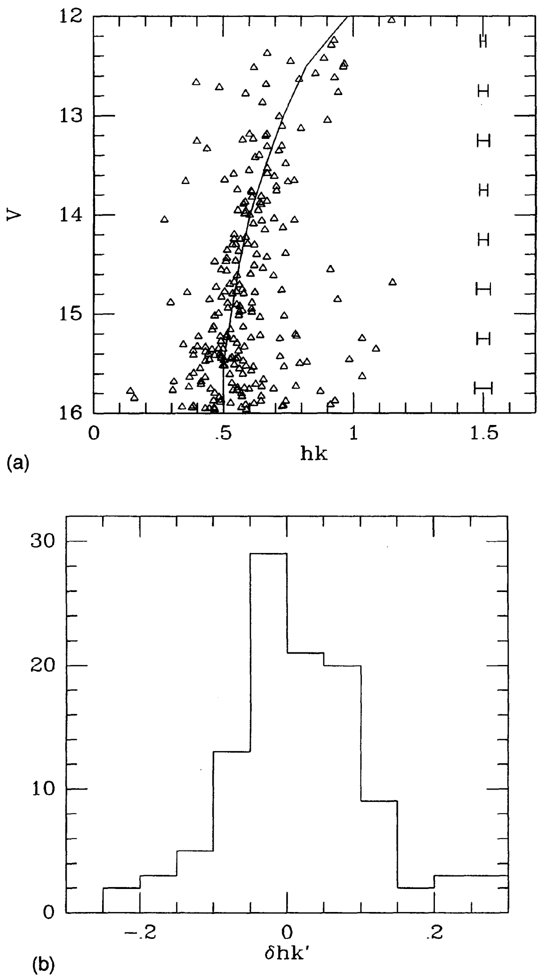

FIG. 11—As for Figs. 6 and 9, but for the hk index. The $\delta hk'$ indices have been normalized to have the same sensitivity as stars at the faint end of the giant-branch sample.

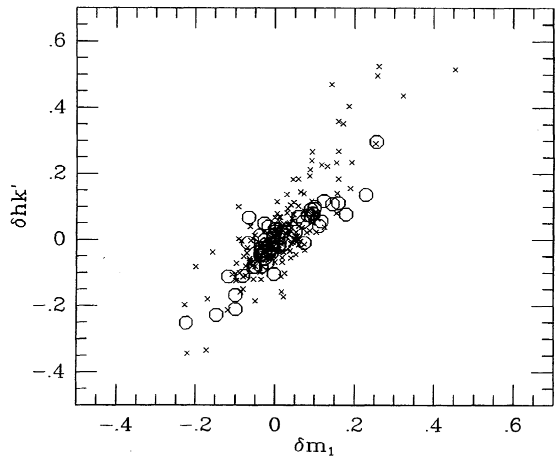

FIG. 12—For the restricted giant-branch sample, the normalized $\delta hk'$ index vs. δm_1. Symbols have the same meaning as Fig. 10.

stars that are metal rich in Ca are metal rich in m_1. Except for a few extreme cases, the stars fill a well-defined range between $\delta hk' = -0.15$ and $+0.15$. Given the results in Sec. 5.1, this implies that the Ca abundance is correlated with the CN/CH strength, exactly the same result found in NF and reconfirmed in Sec. 4.

If the fainter stars without membership information are included, the number of outlying stars increases as expected, but the majority of the points fall within the same well-defined band delineated by the members. From this we conclude that the spreads in Ca and CN/CH extend at least two magnitudes below the horizontal branch and are correlated with each other.

Given the type of correlation seen in Fig. 12, two questions come to mind: First, since hk and m_1 are defined the same way except that the v filter in m_1 is replaced by the Ca filter in hk, is the correlation merely an artifact of common errors in $(b-y)$? Second, if δm_1 within M22 measures CN/CH rather than Fe, is it possible that the hk index is measuring something other than Ca?

The answer to the first question is a definite no. Since the indices can only be linked photometrically through $(b-y)$, large m_1 and large hk are only possible if $(b-y)$ is smaller than expected for a star at a given V, while smaller indices require larger $(b-y)$ than expected. Figure 13 shows δhk as a function of $\delta(b-y)$ for stars at a given magnitude. It is readily apparent that no significant trend exists; a similar result occurs if one plots δm_1 vs. $\delta(b-y)$. Neither the scatter nor the correlation of the indices is caused by photometric errors. It should also be noted that Fig. 13 implies that there is little evidence for a separation of stars in color on the giant branch tied to their overall metallicity, i.e., the more-metal-rich stars do not appear on the redder side of the scatter. If such a trend existed, it would be opposite in slope to the trend predicted by the photometric errors. From Fig. 13 one could argue that a pattern appears to exist for the brighter giants if a pair of outlying points is ignored. We would argue against this interpretation for three reasons: (1) the trend among the brighter giants is itself defined on the basis of less

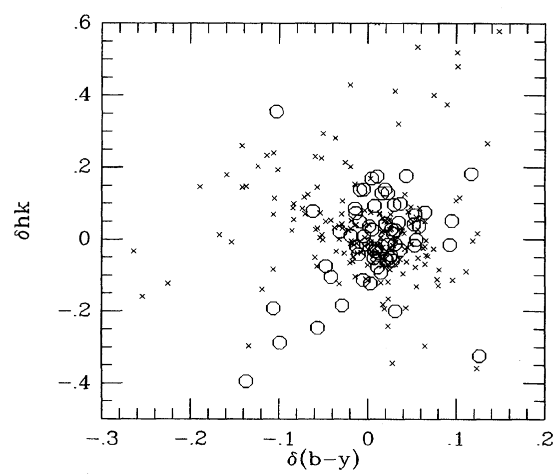

FIG. 13—Plot of $\delta hk'$ and $\delta(b-y)$ for the restricted giant-branch sample. Symbols have the same meaning as Fig. 10.

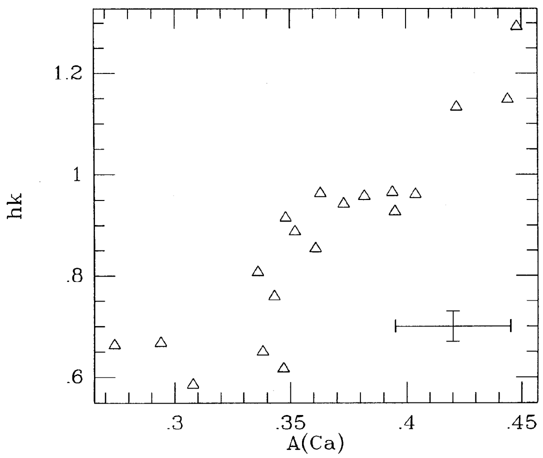

FIG. 14—Comparison of hk index to NF's spectrophotometric index A(Ca) for 19 stars in common with their sample.

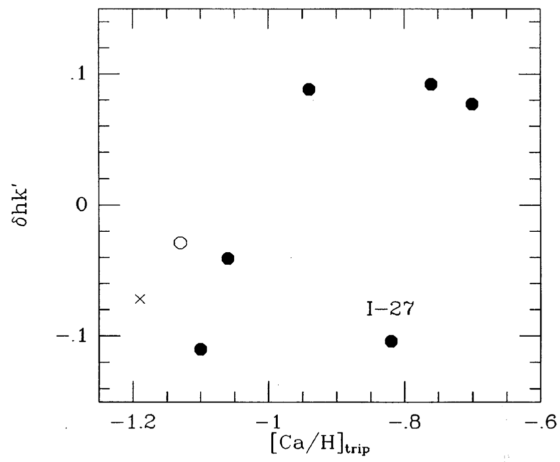

FIG. 15—Comparison of metallicity index $\delta hk'$ to spectroscopic measurements of calcium abundance by LBC; these abundances are derived from the infrared calcium triplet. Symbol meanings are for Fig. 7.

than four points: any pattern whose existence is dependent on the presence or absence of such a small fraction of the entire sample is not reliable. Moreover, the relations among the indices discussed in previous sections are present if all the outlying points are eliminated; the color trend clearly is not; (2) the fainter stars do not exhibit the color trend. While the photometric errors do grow with increasing V, they are not large enough to eliminate a significant color slope if one were present; and (3) the possible slope among the brighter stars is caused by few stars with predominantly negative $\delta(b-y)$, i.e., they have $(b-y)$ indices which are too blue for their magnitude. These stars are easy to identify in Fig. 3(b). They are the stars which appear to fall along the asymptotic giant branch blueward of the giant branch. If these are AGB stars, they are bluer (hotter) intrinsically than the red giants at their V magnitude. The color sensitivity of hk and m_1 is the same; bluer stars at a given [Fe/H] have lower hk and m_1. Thus, these stars will automatically have small δhk and δm_1. If there is a true color dependence among the metallicity indices in Fig. 13, it must be dominated by the scatter in $E(b-y)$ and the photometric errors.

On the second question, there are two pieces of evidence supporting the claim that hk does primarily measure [Ca/H]. First, comparison of the hk index to A(Ca) of NF in Fig. 14 demonstrates that the photometric approach provides the same information as the spectrophotometric index A(Ca), with significantly smaller errors. The central bandpass of the A(Ca) index is narrower (70 Å) than the Ca filter (100 Å) so it should be even more uniquely dependent on [Ca/H] than hk. The most recent calibration of the index by Flynn and Morrison (1990) shows reasonable agreement with standard [Fe/H] values, implying that within the errors [Ca/H] and [Fe/H] are correlated. Second, though the indices appear to be measuring the same thing in the M22 giants, the claim that the key variable is [Ca/H] can only be proven via direct comparison to spectroscopic [Ca/H] determinations; this comparison is shown in Fig. 15. The [Ca/H] abundances are based upon the red Ca triplet rather than the blue lines of Ca II H and K or the weaker Ca lines near 5600 Å and are taken from LBC. The spectroscopic abundances are direct evidence of a spread of 0.4 dex in [Ca/H], a spread which is well correlated with $\delta hk'$ if the probable misidentification of star I-27 by LBC (LBC) is excluded. The unexpected result, however, is the observation that the range in [Ca/H] from $\delta hk'$, 0.8 dex, is about twice the spread predicted from spectroscopy. We conclude that a second parameter, in addition to [Ca/H], is affecting the hk index.

5.3 The Origin of the Anomalies in M22

The photometric analysis of the last two subsections provides irrefutable evidence for significant abundance variations among M22's giants which extend two magnitudes below the horizontal branch and which appear to be interrelated. The remaining, and somewhat surprising, problem is identifying exactly what elements are varying and what their correlations tell us about M22's history. In this section we will attempt to bring together the new results in the context of previous work in M22 as well as in other clusters, and approach a tentative understanding.

On the question of primordial versus internal evolution of the elements, Fe plays a key role; evidence for a significant range in [Fe/H] would be conclusive proof of primordial variation. We had hoped that m_1 for the giants would supply this critical piece of the puzzle. Unfortunately, it is abundantly clear that the m_1 index is dominated through the v filter by some additional source of opacity other than Fe. Though it is possible that some of the spread in δm_1 is a product of a range in [Fe/H], without a better handle on the alternative source, the size of this spread cannot be quantified.

Though we cannot contribute new data to the Fe argument, we can review some of the previous results to better constrain the possibility. One of the first studies to identify a potentially large spread in [Fe/H] among the giants in M22 was the DDO study of Hesser et al. (1977). Using the (3842) combination of DDO filters, which is sensitive to Fe, not CN, they showed that the scatter among the giants was comparable to that found in only one other cluster, ω Cen, and larger than expected from potential reddening variations and photometric errors. However, as noted by Hesser et al. (1977), the spread was dominated by two distinct groups, the first following a well-defined band with modest scatter about the expected mean metallicity of the cluster and a second group of four stars at much higher metallicity. Despite the low galactic latitude, an argument based upon the previous discussion by Arp and Melbourne (1959) was made that contamination of the giant branch by field stars was unlikely. This appears now to be incorrect. Two of the stars, identified as f and D, are 0 probability members in the survey by Peterson and Cudworth (1994). A third star, e, is outside the field of the proper-motion survey, but is a definite nonmember based upon its radial velocity (Lloyd Evans 1978). The fourth star, c, is a possible member based upon its proper motion (72%), but can be excluded due to its radial velocity ((Lloyd Evans 1978). When one considers a possible spread of ± 0.04 in $E(B-V)$ and photometric scatter, the spread in the indices among the remaining group is consistent with no spread in [Fe/H].

Turning to spectroscopic studies, the best constraint to date is provided by LBC who found a mean metallicity for M22 of $[\mathrm{Fe/H}]=-1.54$ with a dispersion of only 0.11 dex based on 10 stars. A sample comparable in size and accuracy is that of Brown and Wallerstein (1992), following up on an earlier analysis of seven giants (Brown et al. 1990). Unfortunately, the Brown and Wallerstein (1992) and LBC studies have only one star in common and utilize different values of the reddening, $E(B-V)=0.42$ in LBC and 0.36 in Brown and Wallerstein (1992). We can place the latter data on the same system as LBC by referring back to the earlier study of Brown et al. (1990); in that paper, the authors attempted to evaluate the impact of variable reddening in M22 by analyzing their spectra under two different assumptions. In one case, all stars were assumed to have $E(B-V)=0.36$; in the second case, stars with potentially higher reddening, as indicated by strong interstellar lines in the spectra, were analyzed assuming $E(B-V)=0.54$. For five stars processed with both reddening values, we have interpolated the size of the change in [Fe/H] if the reddening is increased by 0.06. This adjustment has been added to the values of [Fe/H] given for these stars in the more recent discussion of Brown and Wallerstein (1992). For the two stars processed under the lower reddening assumption alone, a constant offset of 0.05 dex has been adopted. Assuming $E(B-V)=0.42$, the mean [Fe/H] for M22 from seven stars in Brown and Wallerstein (1992) becomes -1.58 with a dispersion of only 0.09 dex. If we average the value for the one star in common and combine the two studies, the cluster mean for 16 stars is $[\mathrm{Fe/H}]=-1.55\pm0.09$.

LBC present results for 10 stars in M13 analyzed with the M22 sample, finding a dispersion in the mean [Fe/H] of ± 0.04. We will assume that this is indicative of the spectroscopic uncertainty for a cluster with no spread in [Fe/H] for both LBC and Brown and Wallerstein (1992), a very conservative estimate. If the derived spread in reddening is applicable to the stars included in the spectroscopic survey, an approximate estimate of the dispersion in [Fe/H] caused by a dispersion in $E(B-V)$ of ± 0.04 is ± 0.035 dex. Combining these, the true dispersion in [Fe/H] among the giants in M22 is ± 0.07 dex. Though it could be argued that the sample is small and potentially unrepresentative, it should be remembered that the stars in both studies were picked to provide examples of the divergent abundances in Ca and CN/CH as identified by NF. If Fe does vary in M22, it varies to a degree which is significantly smaller than either Ca or CN/CH and does not exhibit any correlation with Ca, Na, or CN/CH (LBC).

The next critical element is Ca, critical because its origins have been tied exclusively to nucleosynthesis within high-mass stars, i.e., it is assumed to be primordial. The hk index correlates well with the A(Ca) index of NF, implying that if A(Ca) truly measures Ca abundance variations, so does hk. The most recent calibration of A(Ca) by Flynn and Morrison (1990) supports this claim if [Ca/H] varies monotonically with [Fe/H], in agreement with the direct calibration of the hk index by Twarog and Anthony-Twarog (1991). Direct support for a link between the indices and [Ca/H] in M22 is supplied by the spectroscopic analysis of LBC, who also emphasize an important point about many of the earlier studies. LBC selected their sample to isolate two extreme groups of stars based upon the A(Ca) index. Because of the scatter in the individual indices, it was felt that such a selection would have the greatest probability of identifying a true spread in [Ca/H]. Even with this choice, the range in [Ca/H] was found to be only 0.4 dex. LBC then showed using their calibration of δA(Ca) that the small samples in most of the earlier studies contained too small a range in [Ca/H] to produce a detectable spread. This may also explain why the [Ca/Fe] data of Brown and Wallerstein (1992) show only marginal evidence for a spread in [Ca/H]. From δA(Ca), the range in [Ca/H] among the six stars should be 0.3 dex. However, if only one star is excluded, this spread drops to 0.18 dex with no distinct groupings among the stars. The observed range in [Ca/Fe] among the six stars is 0.24 dex. A similar problem arises in discussions of the ΔS range among the six RR Lyrae variables in M22. Though a spread of 0.5 dex exists in [Ca/H] based upon the range in ΔS, the sample is small and the scatter is not inconsistent with what is expected from the observational errors alone (Butler 1975).

As LBC did, we find that the Ca spread from δA(Ca) is unimodal for stars between $V=11$ and 13. The hk index extends this result to $V=16$, two magnitudes below the horizontal branch, guaranteeing that the stars are first-ascent red giants and severely constraining any attempt to explain the spread via internal mixing, nucleosynthetic questions aside.

Despite the apparent agreement among our data, NF and LBC, one troublesome discrepancy remains with respect to the size of the [Ca/H] spread. The definitive value to date should be that based upon the spectroscopic sample of LBC, 0.4 dex. NF originally estimated a value between 0.25 and 0.5 dex based upon various assumptions for the contributions of different elements to the opacity of the atmosphere. One can try a direct measure of the spread using the recalibration of A(Ca) as a function of $(B-V)_0$ by Flynn and Morrison (1990). The calibration in the range of interest is defined by the mean relations through the data for three clusters, 47 Tuc at [Fe/H]$=-0.8$, NGC 6752 at [Fe/H]$=-1.5$, and NGC 6397 at [Fe/H]$=-2.0$. More recent discussions of cluster abundances (e.g., Anthony-Twarog et al. 1992) indicate that [Fe/H]$=-1.9$ is more appropriate for NGC 6397 while spectroscopic analysis of giants in NGC 6752 leads to [Fe/H] $=-1.58$ for that cluster (Minniti et al. 1992).

Adopting $E(B-V)=0.42$ and using the photographic $(B-V)$ data of NF, the giants of M22 generally follow the $A(\mathrm{Ca})$, $(B-V)$ relation for NGC 6752, in excellent agreement with expectation from the spectroscopic abundance. The data are well bounded at the metal-rich end by 47 Tuc and at the metal-poor end by the approximate curve for [Fe/H]$=-1.7$, implying a range of 0.8 to 0.9 dex. Part of the scatter is due to a combination of photometric scatter in $(B-V)$ and in reddening. Assuming a scatter of ± 0.04 in $E(B-V)$ and ± 0.03 in $(B-V)$ leads to combined scatter of ± 0.05 in $(B-V)_0$. Using the slope of the $A(\mathrm{Ca})$, $(B-V)_0$ relation typical for the giants in M22, this translates into a scatter in $A(\mathrm{Ca})$ of ± 0.014. Combined with a probable error in $A(\mathrm{Ca})$ of ± 0.025 for a single observation, the composite scatter in $A(\mathrm{Ca})$ about the mean relation should be ± 0.029. Before converting this to a spread in [Ca/H] it should be emphasized that the sensitivity of $A(\mathrm{Ca})$ to changes in [Ca/H] is nonlinear, decreasing significantly at higher abundance. Thus scatter toward higher $A(\mathrm{Ca})$ produces a greater change in [Ca/H]. At a color typical of the giants in M22, the spread in [Fe/H] becomes a $+0.5$ and -0.15 dex for an error of $+0.029$ and -0.029 in $A(\mathrm{Ca})$, respectively. Thus, all things being equal, the $A(\mathrm{Ca})$ data of NF are consistent within the errors with a true spread in [Ca/H] of 0.4 dex or less.

Unfortunately, a similar argument cannot be made for hk. As discussed in Sec. 5.2, the errors in hk are significantly smaller than those in $A(\mathrm{Ca})$. Even after taking the errors into account, the spread in [Ca/H] implied by the hk data is greater than 0.8 dex. We are disinclined to believe that the sensitivity of the hk index is a factor of two larger than expected from the calibration based upon field stars and suggest that the hk index is being influenced by a source of opacity not normally found in the average halo field giant. More important, the well-defined correlations between $A(\mathrm{Ca})$ and [Ca/H] require that the opacity source correlate with [Ca/H]. To find the solution we now turn to δm_1 and the CN/CH variations.

As discussed earlier, there is universal agreement among the photometric and spectrophotometric studies that M22 shows rich variations among the CNO elements. The reanalysis of the data of NF highlights the fact that M22 is typical of the globular cluster population in the sense that the distributions in CN and CH are bimodal; approximately 30% of the stars fall within the metal-rich peak. What is atypical, is the correlation between CN and CH. Though unusual, an explanation for this correlation is readily available. Assume that both the C and N abundances are allowed to vary from low to high. If one looks at the extreme combinations, of the four possibilities, only a star which is both C and N rich will produce a CN-strong star. Assume further that the abundances are set so that N is the dominant element of the pair—if C is increased, CN and CH strength increase together, creating a correlation.

Suppose instead that C is dominant, the common assumption for first-ascent giants in globular clusters. If N variations are produced by processing of C to N and mixing of the enriched material to the stellar surface, for modest C depletions the CN strength is increased as N rises. Likewise, such depletions of C will weaken CH, creating the more typical CN–CH anticorrelation. Clearly, this pattern reaches a limit since excessive processing will reverse the C dominance over N and revert to the previous case. Moreover, the observable size of the changes will depend upon the absolute abundance of C and N, not just the relative abundance, and the possible effects of O to N processing. A more detailed and quantitative explanation of these points can be found in Smith (1987, 1992). From this simple analysis, one must conclude that among the giants in M22 N is dominant over C, a result confirmed by the spectroscopic data of Brown et al. (1990). An additional piece of evidence suggesting a high initial abundance of N is provided by the analysis of the dusty planetary nebula 18333$-$2357, a confirmed member of M22 (Cudworth 1990) which shares its high velocity relative to the surrounding galactic environment. Analysis by Borkowski and Harrington (1991) of the PN confirms high abundances of C, O, and Ne, with N the presumed precursor of the Ne in the original low-mass giant. Although it is not what they presume, the authors' analysis is consistent with a large primordial abundance of N.

Are the CN/CH variations primordial or caused by mixing? The evidence to date strongly favors a primordial origin. First, if mixing were the source, it initiated well below the level of the giants in NF because the C to N processing has already tipped the C/N balance in favor of N. The observation that δm_1 is a strong measure of CN/CH strength allows us to push this boundary an additional two magnitudes below the horizontal branch, requiring significant mixing to occur by the base of the giant branch at the latest. Moreover, the combined constraints imposed by the CNO abundances and the $^{12}\mathrm{C}/^{13}\mathrm{C}$ ratios for giants in M22 (Brown et al. 1990) are inconsistent with nuclear processing and mixing alone; the N range among the main-sequence stars also must have been about 1.5 dex with possibly a much smaller spread in C. Second, CN and CH are well correlated with Ca determined from high-dispersion spectroscopy (LBC), spectrophotometry (NF), and photometry. Given the lack of any nonprimordial source of Ca, such a correlation heavily favors a primordial origin for the CN/CH variations. The one note of caution is the observation that while CN and CH have bimodal distributions, Ca does not. If mixing were the source, one could claim that mixing occurred more efficiently for whatever reason in stars which were metal rich. Despite the consistency of the various studies, a key problem remains. The m_1 index through the v filter is dominated by the correlated strength of the CN/CH feature, rather than [Fe/H] as hoped. The spread in m_1 is a factor of 5 to 10 times larger than allowed by the spread in [Fe/H]. This excessive sensitivity is very reminiscent of the problem noted for hk where the range in the index is a factor of two larger than expected. Within the v filter the only obvious link to CN is through the CN 4215 Å band, which lies in the wings of the bandpass; there are no potential links for the Ca filter in hk. As noted in Sec. 5.1, the only halo field giants which exhibit a comparable change in m_1 and c_1 are those classed as CH strong. (A point of clarification is in order. CH-strong stars as discussed here are not meant to imply that these stars are CH subgiants or Ba II stars, classes of stars which also exhibit anomalous m_1, c_1 indices. These stars are generally recognized through the presence of s-process elements and radial-velocity studies as being members of mass-transfer binary systems. CH strong in the present context does not imply either binarity or s-process enhancements, merely a strong G band. For a specific example of this point in M22, see the discussion of star III-106 by Vanture and Wallerstein 1992.) This observation is crucial because the CN bands in these stars are not the source of the photometric anomaly. The only explanation to date remains the mysterious Bond-Neff effect (Bond and Neff 1969), attributed to a source of continuous absorption ranging from at least 3900 to 4100 Å. Whether the opacity is tied to the C abundance directly or indirectly through alteration of the relative abundances of molecules tied to C, N, or O remains unknown. However, it does explain the change in m_1 and the correlated effect on hk. The Ca filter falls within the short wavelength end of the absorption, changing hk in step with the correlated change in Ca and CH. The A(Ca) index is affected weakly, if at all, because the bandpass is compared to continuum bandpasses on either side of Ca II H and K lines. Since the continuum bandpasses are also altered by the Bond-Neff opacity, the differential line strength maintains sensitivity primarily to changes in Ca.

We close this section by attempting to place M22 within the context of abundance variations in other globular clusters, using both our data and the analyses of earlier investigators. For an excellent review of the current state of affairs within the cluster population, the reader is referred to Kraft (1994). The trend that has emerged in recent years is the recognition that there is no universal pattern that applies to all globular clusters. While mixing of nuclear-processed material to the surfaces of evolved giants definitely occurs within some clusters, the amount of such mixing varies from cluster to cluster. The evidence for mixing is based upon linked variations in C, N, and O. Clusters cited as evidence for mixing exhibit variations in C, N, and O which leave C+N+O constant, as expected for processing in evolved giants. Moreover, the relative changes in the elements are often strongly dependent upon evolutionary phase (see, e.g., Suntzeff 1993). An additional argument in favor of mixing is the observation of low ^{12}C/^{13}C ratios among evolved stars (Smith and Suntzeff 1989; Bell et al. 1990; Suntzeff and Smith 1991).

On behalf of primordial variations, the entire cluster population provides evidence for abundance variations which are not predicted by standard mixing theory, either in type, amount or evolutionary phase. By far, the strongest arguments are tied to the presence of variable CN strength among stars from the base of the giant branch to the turnoff in 47 Tuc (Bell et al. 1983) and NGC 6752 (Suntzeff 1989). In some clusters (Briley et al. 1989, 1992) the CN abundances are not consistent with all stars having the same initial C+N abundance. Until recently, a common argument in favor of the need for primordial variations has been the observed correlation between N, Na, and Al, and the observed anticorrelation between O and Na, nucleosynthetic connections that could not be produced in evolving low-mass giants. This barrier has been partially breached with the work of Denisenkov and Denisenkova (1990) and Langer et al. (1993), while the observational evidence of Kraft et al. (1993) for M13 indicates that the O–Na anticorrelation only becomes excessive, i.e., super-oxygen-poor stars can only be found at high luminosities. If correct, this implies that the relationship between Na and O found for a large sample of bright giants in all clusters studied to date (Kraft et al. 1993) is a product of mixing, again occurring to different degrees in different clusters, potentially controlled by stellar rotation.

How does M22 fit into this picture? Brown and Wallerstein (1992) have shown that the ^{12}C/^{13}C ratio among the giants is low, as predicted following mixing on the giant branch; mixing has occurred in M22. However, neither C+N+O nor C+N are constants; the analysis by Brown et al. (1990) implies that N variations were already present among the giants in M22 before any mixing occurred. A spread in [O/Fe] is present among the giants, though none of the seven stars in Brown et al. (1990) classifies as being super-oxygen poor, a pattern similar to that in M3. A spread in [Na/Fe] of about 0.8 dex is present in the samples of both Brown and Wallerstein (1992) and LBC; Brown and Wallerstein (1992) find that CN, Na, and Al are correlated, as observed in other clusters. While the spread in [O/Fe] and the links between CN, Na, and Al are consistent with the mixing proposal of Kraft et al. (1993), the observed correlation between Ca and Na found by LBC is not. As noted earlier, production of Ca is not consistent with standard low-mass red giant evolution and mixing (an obvious caveat is that the same argument has been used regularly for Na). If Ca variation is primordial and Na is correlated with Ca, either the Na variations are primordial or the efficiency of mixing is somehow correlated with the metallicity of the evolving giant, i.e., Ca-rich stars mix more than Ca-poor stars. However, if the primordial overabundance of N is the source of the spread in C+N+O, it is unlikely that mixing produces the correlations between Na and CN. Since N dominates, CN strength is controlled by the C abundance. Stars with strong CN have undergone less mixing, not more. If mixing results in higher Na, Na should be anticorrelated with CN, the opposite of what is observed. It is concluded that while mixing does exist among the giants of M22, the predominant variations in abundance, those of Ca, CN, and, possibly Na, have their origins in a primordial mechanism and should extend to stars on the main sequence.

6. CONCLUSIONS AND FUTURE WORK

CCD *uvbyCa* photometry of M22 extending two magnitudes below the horizontal branch has been presented and a select subset of probable members with high photometric accuracy has been analyzed. Over the cluster fields studied, the color spread in $(b-y)$ for the definite members of the giant branch and the blue horizontal branch indicates that the cluster suffers a real but modest [± 0.04 mag in $E(B-V)$] variation in reddening. After removing the effects of reddening and photometric error, little room remains for any intrinsic spread in color caused by a range in [Fe/H], though a spread of less than 0.2 dex cannot be excluded.

Using m_1 and hk, it is apparent that a significant variation does exist among the giants for both CN/CH and Ca and that the variations are positively correlated. The δhk index is shown to be well correlated with the δA(Ca) index of NF, while δm_1 is tied to $\delta S(3839)$ and δW(G). The spread in m_1 is more than five times larger than predicted from the spectroscopic [Fe/H] and the hk range is twice as large as predicted from [Ca/H]. It is concluded that the giants in M22 exhibit an anomalous opacity at shorter wavelengths analogous to the Bond-Neff effect seen in CH-strong stars. This dominates the variation in m_1 through the v filter, but superposes upon the comparable range caused by the spread in Ca on the Ca filter. The presence of this anomaly appears tied to the fact that CN and CH are positively correlated in M22. Reanalysis of the data of NF demonstrates that both CN and CH have bimodal distributions while Ca does not. While mixing must occur to some degree among the giants, the variation of Ca, the excessive range in N, and the observation of variations almost to the base of the giant branch are best explained as being primordial in origin.

Though the observations obtained in this investigation have hopefully clarified and better defined the reality of abundance variations in M22, the underlying questions regarding their origin remain unanswered. Major stumbling blocks for both sides of the mixing/primordial argument are the mechanisms which lead to a range from cluster to cluster and from star to star within a cluster. Why are CN variations bimodal? How does one produce a primordial range in CN without affecting the range in [Fe/H] as in 47 Tuc, or a range in CN and Ca without altering [Fe/H] as appears to be the case in M22? If the variations are primordial in M22, are they caused by the retention of gas from a first generation of Type II or Ia SNe, or some less violent form of mass loss and/or stellar wind (Brown and Wallerstein 1992). The former explanation is not strengthened by the rather average mass of M22 compared to the excessively high mass of ω Centauri. It is likely that the primordial position cannot be tested without observations of the key elements of Fe, Ca, C, N, O, and Na extending to the main sequence. Photometric data which will allow a test of the Ca spread at the turnoff have already been obtained.

On a slightly different issue, the possible presence of the Bond-Neff opacity among the giants in M22 raises a problem which remains unsolved 25 years after it was first noted (Bond and Neff 1969), i.e., what is it? Because the effect has been apparent in only a small subset of peculiar stars, the exact nature of its source has been a question of low priority. If the Bond-Neff opacity is the cause of the excessive sensitivity of the indices in M22, it implies that the size of the opacity effect can cover a wide range but may only be obvious in stars at the extreme end of the continuum. A potential link to the broader sample of field stars arises from a comparison to two of the more extreme halo giants, CD $-38°245$ and BD $-18°5550$ (Twarog and Anthony-Twarog 1991). It has been shown that the photometry of these two giants at the blue end is distorted by the presence of some continuum source similar to the Bond-Neff opacity. The effect of this opacity, which is strong in CD $-38°245$, is to make this star appear anomalously metal rich on the DDO, Washington, *uvby, Caby*, and Geneva systems. In contrast, BD $-18°5550$ is anomalously metal weak. From ultraviolet spectra of these giants, Anthony-Twarog et al. (1992) found that the variation in the opacity is tied to the abundance of N; N is grossly overabundant in CD $-38°245$ and almost absent in BD $-18°5550$. The spread and the excess of N in M22 may have links to nucleosynthesis among the first generation of stars in the Galaxy.

University of Kansas undergraduate Jennifer Hand cheerfully assisted with data reductions. Conversations with Ruth Peterson were extremely helpful in expanding the discussions. Comments by the referee led to a number of useful clarifications. We gratefully acknowledge the support provided by the University of Kansas and the Department of Physics and Astronomy, and the generous allocation of resources by the Cerro Tololo Inter-American Observatory. The research of one of us (J.S.C.) was supported in part by funds from the National Science Foundation, through the American Astronomical Society's REU program.

REFERENCES

Alcaino, G. 1977, A&AS, 29, 383

Alcaino, G., and Liller, W. 1983, AJ, 88, 1330

Anthony-Twarog, B. J. 1987, AJ, 93, 1454

Anthony-Twarog, B. J., Laird, J. B., Payne, D., and Twarog, B. A. 1991, AJ, 101, 1902

Anthony-Twarog, B. J., Shawl, S. J., and Twarog, B. A. 1992, AJ, 104, 2229

Anthony-Twarog, B. J., and Twarog, B. A. 1994, AJ, 107, 1577

Anthony-Twarog, B. J., Twarog, B. A., and Sheeran, M. E. 1994, PASP, 106, 486

Anthony-Twarog, B. J., Twarog, B. A., and Suntzeff, N. B. 1992, AJ, 103, 1264

Arp, H. C., and Melbourne, W. G. 1959, AJ, 64, 28

Ashman, K. M., Bird, C. M., and Zepf, S. E. 1994, AJ, 108, 2348

Bates, B., Montgomery, A. S., Wood, K. D., Davies, R. D., and Walker, H. J. 1992, MNRAS, 287, 699

Beers, T. C., Preston, G. W., and Shectman, S. A. 1985, AJ, 90, 2089

Beers, T. C., Preston, G. W., and Shectman, S. A. 1992, AJ, 103, 1987

Bell, R. A., Briley, M. M., and Smith, G. H. 1990, AJ, 100, 187

Bell, R. A., Hesser, J. E., and Cannon, R. D., 1983, ApJ, 269, 580

Bond, H. E. 1980, ApJS, 44, 517

Bond, H. E., and Neff, J. S. 1969, ApJ, 158, 1235

Borkowski, K. J., and Harrington, J. P. 1991, ApJ, 379, 168

Briley, M. M., Bell, R. A., Smith, G. H., and Hesser, J. E. 1989, ApJ, 341, 800

Briley, M. M, Smith, G. H., Bell, R. A., Oke, J. B., and Hesser, J. E., 1992, ApJ, 387, 612

Briley, M. M., Smith, G. H., Hesser, J. E., and Bell, R. A. 1993, AJ, 106, 142

Brown, J. A., Wallerstein, G., and Oke, J. B. 1990, AJ, 100, 1561

Brown, J. A., and Wallerstein, G. 1992, AJ, 104, 1818

Butler, D. 1975, ApJ, 200, 68

Crocker, D. A. 1988, AJ, 96, 1649
Cudworth, K. M. 1990, AJ, 99, 1863
Cudworth, K. M. 1986, AJ, 92, 1986
Denisenkov, P. A., and Denisenkova, S. N. 1990, Sov. Astron. Lett., 16, 275
Dickens, R. J., and Wooley, R. v. d. R. 1967, ROB, No. 128
Flynn, C., and Morrison, H. L. 1990, AJ, 100, 1181
Frogel, J. A., Persson, S. E., and Cohen, J. G. 1983, ApJS, 53, 713
Gustafsson, B., and Bell, R. A. 1979, A&A, 74, 313
Hesser, J. E. 1976, PASP, 88, 849
Hesser, J. E., and Harris, G. L. H. 1979, ApJ, 234, 513
Hesser, J. E., Hartwick, F. D. A., and McClure, R. D. 1977, ApJS, 33, 471
Kraft, R. P. 1994, PASP, 106, 553
Kraft, R. P., Sneden, C., Langer, G. E., and Shetrone, M. D. 1993, AJ, 106, 1490
Kurucz, R. L. 1991, in Precision Photometry: Astrophysics of the Galaxy, ed. A G. D. Philip, A. R. Upgren, and K. A. Janes (Schenectady, Davis), p. 27
Laird, J. B., Wilhelm, R. J., and Peterson, R. C. 1991, in The Formation and Evolution of Star Clusters, ed. K. A. Janes (San Francisco, ASP), p. 578
Langer, G. E., Hoffman, R., and Sneden, C. 1993, PASP, 105, 301
Lehnert, M. D., Bell, R. A., and Cohen, J. G. 1991, ApJ, 367, 514 (LBC)
Lloyd Evans, T. 1978, MNRAS 182, 293
Luck, R. E., and Bond, H. E. 1982, ApJ, 259, 792
Luck, R. E., and Bond, H. E. 1991, ApJS, 77, 515
Minitti, D., Coyne, G. V., and Claria, J. J. 1992, AJ, 103, 871
Mukherjee, K., Anthony-Twarog, B. J., and Twarog, B. A. 1992, PASP, 104, 561
Norris, J., and Freeman, K. C. 1983a, ApJ, 266, 130 (NF)
Norris, J., and Freeman, K. C. 1983b, ApJ, 273, 838 (NF)
Peterson, R. C., and Cudworth, K. M. 1994, ApJ, 420, 612
Pilachowski, C. A., Sneden, C., and Booth, J. 1993, ApJ, 407, 699
Schechter, P. L., Mateo, M., and Saha, A. 1993, PASP, 105, 1342
Schuster, W. J., and Nissen, P. E. 1989, A&A, 221, 65
Smith, G. H. 1987, PASP, 99, 67
Smith, G. H. 1992, PASP, 104, 894
Smith, V. V., and Suntzeff, N. B. 1989, AJ, 97, 1699
Soon, W. H., Zhang, Q., Baliunas, S. L., and Kurucz, R. L. 1993, ApJ, 416, 787
Suntzeff, N. B. 1989, in The Abundances Spread Within Globular Clusters, ed. G. Cayrel de Strobel, M. Spite, and T. Lloyd Evans (Paris, Obs. de Paris), p. 71
Suntzeff, N. B. 1993, in The Globular Cluster—Galaxy Connection, ASP Conference Series, Vol. 48, ed. G. H. Smith and J. P. Brodie (San Francisco, ASP), p. 167
Suntzeff, N. B., and Smith, V. V. 1991, ApJ, 381, 160
Tripicco, M. J., and Bell, R. A. 1991, AJ, 102, 744
Twarog, B. A., and Anthony-Twarog, B. J. 1991, AJ, 101, 237
Twarog, B. A., and Anthony-Twarog, B. J. 1995, AJ, submitted
Vanture, A. D., and Wallerstein, G. 1992, PASP, 104, 888